Annals of Botany **109**: 1133–1148, 2012
doi:10.1093/aob/mcs042, available online at www.aob.oxfordjournals.org

ANNALS OF BOTANY
Founded 1887

Extreme phenotypic variation in *Cetraria aculeata* (lichenized Ascomycota): adaptation or incidental modification?

Sergio Pérez-Ortega[1,*], Fernando Fernández-Mendoza[2,3], José Raggio[4], Mercedes Vivas[4], Carmen Ascaso[1], Leopoldo G. Sancho[4], Christian Printzen[2,3] and Asunción de los Ríos[1]

[1]*Museo Nacional de Ciencias Naturales, MNCN-CSIC, c/ Serrano 115 dpdo, E-28006 Madrid, Spain,* [2]*Senckenberg Research Institute, Department of Botany and Molecular Evolution, Senckenberganlage 25, D-60325 Frankfurt am Main, Germany,* [3]*Biodiversity and Climate Research Center, Senckenberganlage 25, D-60325 Frankfurt am Main, Germany and* [4]*Departamento de Biología Vegetal II, Facultad de Farmacia, Universidad Complutense de Madrid, Pza. Ramón y Cajal S/N, 28040 Madrid, Spain*

** For correspondence. E-mail sperezortega@mncn.csic.es*

Received: 7 September 2011 Returned for revision: 31 October 2011 Accepted: 2 February 2012 Published electronically: 25 March 2012

• *Background and Aims* Phenotypic variability is a successful strategy in lichens for colonizing different habitats. Vagrancy has been reported as a specific adaptation for lichens living in steppe habitats around the world. Among the facultatively vagrant species, the cosmopolitan *Cetraria aculeata* apparently forms extremely modified vagrant thalli in steppe habitats of Central Spain. The aim of this study was to investigate whether these changes are phenotypic plasticity (a single genotype producing different phenotypes), by characterizing the anatomical and ultrastructural changes observed in vagrant morphs, and measuring differences in ecophysiological performance.

• *Methods* Specimens of vagrant and attached populations of *C. aculeata* were collected on the steppes of Central Spain. The fungal internal transcribed spacer (ITS), glyceraldehyde-3-phosphate dehydrogenase (GPD) and the large sub-unit of the mitochondrial ribosomal DNA (mtLSUm), and the algal ITS and actin were studied within a population genetics framework. Semi-thin and ultrathin sections were analysed by means of optical, scanning electron and transmission electron microscopy. Gas exchange and chlorophyll fluorescence were used to compare the physiological performance of both morphs.

• *Key Results and Conclusions* Vagrant and attached morphs share multilocus haplotypes which may indicate that they belong to the same species in spite of their completely different anatomy. However, differentiation tests suggested that vagrant specimens do not represent a random sub-set of the surrounding population. The morphological differences were related to anatomical and ultrastructural differences. Large intercalary growth rates of thalli after the loss of the basal–apical thallus polarity may be the cause of the increased growth shown by vagrant specimens. The anatomical and morphological changes lead to greater duration of ecophysiological activity in vagrant specimens. Although the anatomical and physiological changes could be chance effects, the genetic differentiation between vagrant and attached sub-populations and the higher biomass of the former show fitness effects and adaptation to dry environmental conditions in steppe habitats.

Key words: Diffuse-intercalary growth, lichens, *Cetraria aculeata*, Ascomycota, phenotypic variability, spatial disturbance, ultrastructure.

INTRODUCTION

Phenotypic plasticity is the capacity of a given genotype to develop different phenotypes under different environmental conditions (Bradshaw, 1965; Valladares *et al.*, 2007). This capacity is especially valuable for sessile organisms such as plants or fungi because it allows establishment and survival in sub-optimal habitats (Bradshaw, 1965; Sultan, 2000). Numerous studies have shown that ecologically important traits such as morphology, anatomy, physiology and reproduction are plastic in lichens (e.g. Larson, 1989; Nash *et al.*, 1990; Pintado *et al.*, 1997; Rikkinen, 1997; Sojo *et al.*, 1997; Jackson *et al.*, 2006).

Lichens show adaptations to different ecosystems. Anatomical and physiological adaptations displayed by species of cold or coastal fog deserts are well documented (e.g. Rundel, 1978; Kappen, 1982, 2000; Lange *et al.*, 2008). Some studies have also shown the infraspecific adaptation of lichen populations to different microhabitats (e.g. Tretiach and Brown, 1995; Pintado *et al.*, 1997; Sojo *et al.*, 1997; Plusnin, 2004).

Vagrant lichens, with almost 100 lichenized fungal species recorded worldwide, represent one of the most striking morphological modifications and adaptations to a specific environment (Elenkin, 1901; Weber, 1977). They are known from different taxonomical groups and can be found living in such different ecosystems as saltbush country in Australia, the Eurasian steppes, Arctic tundra, North American short-grass prairie, the Atacama and Namib coastal fog deserts, or the Andean Paramo (Weber, 1977; Rosentreter, 1993; Pérez, 1997). These environments share similar arid or semi-arid climatic conditions, and are sparsely vegetated and wind

swept (Weber, 1977; Rosentreter, 1993). Vagrant lichens can be differentiated into strictly vagrant species that only live unattached and species that usually live terricolous or saxicolous but may become vagrant in particular environments. Studies on strictly vagrant lichens have investigated morphological and anatomical adaptations (Büdel and Wessels, 1986; Lumbsch and Kothe, 1988; Pérez, 1997), physiology (Sancho *et al.*, 2000), dispersal capacity (Eldridge and Leys, 1999) and, more recently, the evolution of vagrancy in the foliose lichen genus *Xanthoparmelia* (Leavitt *et al.*, 2011*a*, *b*). However, few studies have focused on the differences between attached and vagrant morphs of optionally vagrant lichens and the physiological implications of these differences (Weber, 1977; Kunkel, 1980; Leavitt *et al.*, 2011*a*, *b*).

Cetraria aculeata (Schreb.) Fr. is a terricolous lichen species, forming shrubby tufts in a wide variety of biomes and microhabitats worldwide (Kärnefelt, 1979; Fernández-Mendoza *et al.*, 2011). It is a morphologically variable species in size, width and colour of its terete to slightly flattened branches, the structure of the pseudocyphellae of the cortex that facilitate gas exchange and the frequency of thallus projections. This variability has led to the description of numerous species and infraspecific taxa, which display, however, continuous variation (Kärnefelt, 1979). An exceptional case of putative phenotypic variability within *C. aculeata* occurs on the steppes of Central Spain (called '*parameras*'). There, *C. aculeata* becomes vagrant and undergoes drastic modifications in morphology, to the extent that these morphs have been assigned to a different species, *C. steppae* (Savicz) Kärnefelt, represented in some Spanish herbaria (MA, MAF and MACB).

Such a substantial modification of thallus morphology, as well as modification of its usual ecology (attached vs. vagrant), raises many questions about the genetic isolation between vagrant and attached specimens, the anatomical background of these modifications, the possible differences in the ecophysiology of both morphotypes, or the relative frequency of such modifications in natural populations. Here, we show the results of a study considering several aspects of the biology of the vagrant morphs of *C. aculeata* in the steppes of Central Spain. We aim to answer the following questions. (1) Do vagrant forms identified as *C. aculeata* belong genetically to *C. aculeata*? (2) Do the bionts involved in the symbiosis in both attached and vagrant morphotypes share haplotypes or do vagrant and attached morphs differ in photobiont use? (3) Which anatomical modifications distinguish vagrant morphs of *C. aculeata* from attached morphs and how are these modifications achieved? (4) What is the frequency of these vagrant morphs in natural populations in steppe regions of Central Spain? (5) Are there noticeable differences in physiological traits such as CO_2 exchange or hydric relationships between both morphotypes?

MATERIALS AND METHODS

The species and taxon sampling

Cetraria aculeata is a fruticose, terricolous lichen that is known from temperate, boreal and arctic regions in the Northern Hemisphere to the Andes, maritime Antarctica, Australia and New Zealand in the Southern Hemisphere (Kärnefelt, 1986; Fernández-Mendoza *et al.*, 2011). A thorough description of the species can be found in Kärnefelt (1986) (under *Coelocaulon aculeatum*).

Specimens were collected in three different sites at the Spanish Central Plateau: Calatañazor (Soria) 41°41′20″N, 2°46′39″W, 1083 m asl; Iruecha (Soria) 41°8′35″N, 2°7′37″W, 1212 m asl; and Zaorejas (Guadalajara) 40°43′55″N, 2°12′45″W, 1278 m asl. The three localities show a rather continental climate, characterized by low winter temperatures (average coldest month: 2 °C) and hot summers (average warmest month: 20 °C); yearly precipitation is approx. 500 mm and shows a pronounced seasonality, with the highest precipitation in winter and spring. The three sites are often swept by strong winds. Bioclimatically they are included in the calcicolous supra-Mediterranean semi-arid vegetation (Rivas-Martínez *et al.*, 2002). The vegetation is dominated by *Juniperus thurifera*, which forms a sparse forest. The lichen flora of this area has been studied by Crespo and Barreno (1978).

Representative thalli of attached and vagrant morphs of *C. aculeata* were sampled in each site (five specimens of each morph in each locality) at irregular intervals on areas of about 2500 m^2 at each locality. Thalli were only collected if more than 0·5 m from another thallus in order to avoid collecting clonal offspring of fragmented thalli. A total of 30 thalli used in the molecular and ecophysiological studies are deposited in the herbarium FR (see Supplementary Data Table S1 and Fig. 1A for information on the sites used in the molecular analysis).

Molecular studies

Samples were prepared and DNA extracted as described in Fernández-Mendoza *et al.* (2011). We used five genetic markers in our study. For the mycobiont, the internal transcribed spacer region of the nuclear ribosomal DNA (ITS), a partial sequence of the large sub-unit of the mitochondrial ribosomal DNA (mtLSU) and a fragment of glyceraldehyde-3-phosphate dehydrogenase (GPD) were used. For the photobiont, the ITS regions and a part of the actin gene were used. DNA isolation, amplification, purification and sequencing follow Fernández-Mendoza *et al.* (2011). The primers and PCR conditions are listed in Supplementary Data Table S2.

The sequences were aligned in Geneious v5·3 (Drummond *et al.*, 2010) using a wrapper for Muscle 3·8 (Edgar, 2004). Ambiguous positions were excluded manually from the sequences; no ambiguous regions were found in the alignment. The photobiont data sets are more variable and more prone to homoplasy (Fernández-Mendoza *et al.*, 2011), making it more difficult to delete ambiguously aligned positions. One sequence of each new haplotype was submitted to GenBank (Supplementary Data Table S3).

Five single gene data sets were assembled for this study: fungal ITS (A), fungal GPD (B), fungal mtLSU (C), algal ITS (D) and algal actin (E). The data sets were built by merging the newly sequenced populations and the data published by Fernández-Mendoza *et al.* (2011) which represent a wider fraction of the geographic range of *C. aculeata*

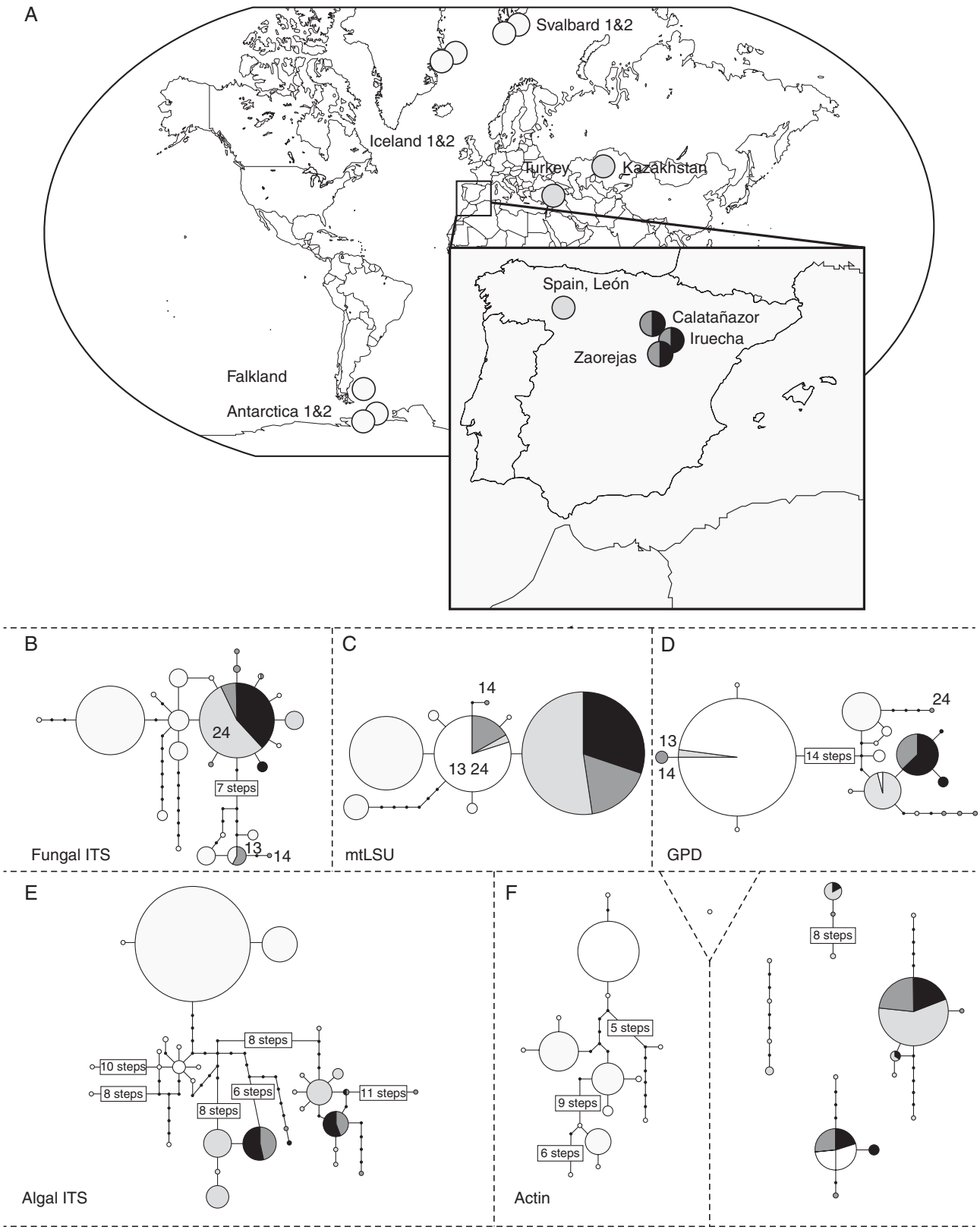

FIG. 1. (A) Sampling localities for populations of *C. aculeata* used in this study. (B) The 90 % parsimony probability haplotype networks constructed from data sets A–H. The size of the circles is proportional to the number of individuals that belong to the respective haplotype. The photobiont actin network falls into five unconnected sub-networks and one single haplotype. The shading in (A) and (B) denotes the geographic origin of the individuals and their sampling scheme: white, polar; light grey, previously sampled Mediterranean *C. aculeata* and *C. steppae*; dark grey, newly collected attached morphs; black, newly collected vagrant morphs.

(Antarctica, Chile, Falkland, Svalbard, Iceland, Spain and Turkey) and include specimens with a norstictic acid chemotype (=*C. steppae*) collected in Kazakhstan. From the published data set, 99 individuals for which the three fungal genes were available and 118 for which the two algal genes were available were included.

As no well-supported (posterior probability ≥0·95) incongruencies were found in the independent data sets of Fernández-Mendoza *et al.* (2011) we concatenated the data sets into two combined data sets, a fungal ITS–mtLSU–GPD data set (F) and an algal ITS–actin data set (G). The data sets are summarized in Supplementary Data Table S2.

Phylogenetic reconstruction. Phylogenetic trees were built for the concatenated mycobiont (F) and photobiont (G) data sets within a Maximum Likelihood (ML) and a Bayesian inference framework. The data sets were collapsed into concatenated multilocus genotypes to avoid pseudoreplication in phylogenetic reconstruction. Even though all phylogenies are unrooted, they are represented as midpoint rooted graphs. The ML analysis was carried out using RaxML v. 7·2·8 (Stamatakis *et al.*, 2005) through the RaxMLGUI v. 0·95 interface (Silvestro and Michalak, 2012). Support values for the topology were calculated using a bootstrap approach averaging >10 runs of 1000 iterations each. Bayesian inference was carried out using the MCMC framework implemented in the program MrBayes, v. 3·2 (Ronquist and Huelsenbeck, 2003). Optimal substitution models were inferred for each marker using jModeltest v. 2·3 (Posada, 2008), and they are summarized in Supplementary Data Table S2.

The Bayesian analyses were run using default priors. The results were summarized over five independent runs with four incrementally heated chains. The parameter distribution was sampled every 1×10^4 tree, and convergence of the chains was assessed during the run by calculating the average standard deviation of split frequencies (SDSF). The convergence of Markov chain parameters was further investigated using potential scale reduction factor (PSRF) criteria as implemented in MrBayes v. 3·2 (Ronquist and Huelsenbeck, 2003) by using the program Tracer v. 1·5 (Rambaut and Drummond, 2010) and the online version of the AWTY program (Nylander *et al.*, 2004).

For the concatenated photobiont data set (G), five independent runs with four incrementally heated chains were started and the same run settings used as in the previous analysis but with default heating value and sampling every 1×10^4 tree. Convergence was tested as above. Using these priors and settings, the chains were run for $12{\cdot}5 \times 10^6$ generations, after which the standard deviation of split frequencies had reached a value of 0·035. A consensus tree was calculated from the $5{\cdot}7 \times 10^3$ post-burnin trees. Trees and data sets were deposited in TreeBase (Treebase ID 12160) Phylogenetic reconstruction methods assume that ancestral nodes are no longer present in the data set and that the evolution of the data set follows a bifurcating pattern. Infraspecific data sets usually do not fulfil these assumptions. We therefore also calculated 95 % parsimony probability haplotype networks for all single gene data sets using TCS v. 1·21 (Clement *et al.*, 2000).

Population genetics. The genetic structure of the vagrant and attached morphs, treated as separate populations, was surveyed and compared using a traditional framework in statistical genetics. For the analysis, a sub-set of the fungal data sets (A–C, F) was used which included only the 30 thalli collected in localities with vagrant and attached morphs growing intermixed. Population structure was described in terms of nucleotide diversity (π; Nei, 1987). Gene flow and genetic isolation between populations was surveyed by means of pairwise F_{ST} (Lynch and Crease, 1990). Statistical significance was assessed via a permutation test (1000 permutations). Genetic differentiation was assessed in terms of average number of nucleotide substitutions per site (D_{xy}) (Nei, 1987) and the exact test for genetic differentiation (Raymond and Rousset, 1995) based on haplotype frequencies. To assess whether the populations of vagrant and attached *C. aculeata* conformed to well differentiated genetic entities, analysis of molecular variance (AMOVA; Excoffier *et al.*, 1992) was carried out on the concatenated and the single gene data sets using the JC69 nucleotide substitution model (Jukes and Cantor, 1969) as distance metric. Statistical significance of the AMOVAs was assessed using randomization tests based on 10^3 permutations. For the calculations of D_{xy} and π, DnaSP v. 5 (Librado and Rozas, 2009) was used. DnaSP was also used to convert the data set for its use in Arlequin v. 3·5 (Excofier and Lischer, 2010) to calculate pairwise F_{ST}s, AMOVAs and the exact test of population differentiation. To test if the vagrant population represents a random sub-sample of the neighbouring attached population, we performed a randomization test on the concatenated data set. A random selection of 10^3 sub-samples with replacement of 15 individuals from the attached and vagrant pools was used. For each group and each re-sampling, the average value of the pairwise JC69 genetic distances was calculated. The distribution of average genetic distances between the two groups using one- and two-tailed *t*-tests was compared. Alternatively, the same analysis was made by stratifying the resampling by location (five samples from each locality). The randomization analysis was implemented in R (R Development Core Team, 2009) using a custom script and aided by basic functions of the *base* package, and packages *pegas* (Paradis, 2010) and *ape* (Paradis *et al.*, 2004).

Morphology, anatomy and ultrastructure

Specimens were examined using a Leica S8APO stereomicroscope fitted with a Leica EC3 image capture system. Samples for ultrastructural and anatomical study were prepared following de los Ríos and Ascaso (2002). In brief, small thallus fragments were initially fixed in glutaraldehyde and thereafter in osmium tetroxide; then dehydrated in a graded ethanol series before embedding in Spurr's resin. Semi-thin (0·35 μm) and ultrathin sections (70 nm) were made on a Reichert Ultracut-E ultramicrotome (using a diamond knife). Ultrathin sections were post-stained with lead citrate (Reynolds, 1963) and observed in a Zeiss EM910 transmission electron microscope.

Semi-thin sections were stained with methylene blue and observed in a Zeiss® AX10 microscope fitted with 'Nomarski' differential interference contrast and a Zeiss® AxioCam digital camera. Measurements of the thickness of thallus layers as well as the compactness of the algal layer were made by means of the Zeiss® Axiovision 4·8 image

analyser system. The density of photobiont cells in the algal layer was calculated using pictures taken at ×630 magnification. The algal layer was defined by two parallel lines tangent to the most external algal cells found in the layer. Density was calculated as the sum of all the areas of photobiont cells in the algal layer, divided by the area comprised between the two parallel lines. Areas were calculated using the Zeiss® Axiovision 4·8 image analyser system. Once the ultrathin sections were taken, the surface of the resin block with the sample remnant was carbon coated and studied by scanning electron microscopy in back-scattering electron mode (BSE-SEM) with a DMS 960 Zeiss microscope.

Chemistry

In order to test for the presence of *C. steppae* in the studied material, we tested the 30 samples used in the molecular and ecophysiological studies for the presence of norstictic acid using thin-layer chromatography (TLC) on glass plates (solvents A and C) following Orange *et al.* (2001).

Biomass analysis

Biomass of *C. aculeata* morphs was estimated in the three study localities using a simplified approach. In each locality, we selected a homogeneous plot of 50 × 50 m, avoiding slopes, proximity of trees or the presence of small seasonal ponds. In each plot, 25 quadrats of 50 × 50 cm were distributed along two transects corresponding to the diagonals of the plot. Every single thallus of any morph of *C. aculeata* occurring in these quadrats was collected into paper bags and carried to the lab. Thalli were carefully cleaned under a compound microscope to remove all plant debris and other lichen fragments. For each thallus, we measured the width of the broadest lobe (to its nearest 0·5 mm) and the weight of the thallus (to its nearest 0·01 g) after oven-drying overnight at 105 °C. For each size class ($X \leq 1{\cdot}5$ mm, 'attached morphs'; $1{\cdot}5 < X \leq 3$ mm, 'intermediate vagrant morphs'; $X >$ 3 mm, 'vagrant morphs') we obtained the average biomass (in kg ha^{-1}) and the standard error. Calculations were made in R (R Development Core Team, 2009).

Water storage capacity and gas exchange

Fifty thalli of each morphotype were chosen among the specimens collected during the biomass experiment, avoiding intermediate forms. Thalli were submerged in sterile water for 20 min, excess water was removed using blotting paper, and they were immediately weighed. Then, the dry thallus was weighed after oven-drying overnight at 105 °C. Water content was calculated as (wet lichen weight – dry lichen weight)/dry lichen weight and given as percentage by weight (Pérez, 1997).

Attached morphs and vagrant morphs were studied separately for CO_2 exchange under controlled laboratory conditions. An open flow IRGA system (CMS 400, Walz, Germany) was used: CO_2 exchange was measured as the difference between the air passed through the cuvette with the lichen and the ambient air (Sancho and Kappen, 1989). Lichen thalli were reactivated for 72 h in a chamber with 12 h light (100 μmol photon m^{-2} s^{-1})/12 h dark, 10 °C, and were sprayed once a day with spring water. Then, in order to assess the response to light, photosynthetic photon flux density (PPFD) response curves were determined: measurements were made at 0, 400, 800 and 1200 μmol photon m^{-2} s^{-1}. These were repeated at 5, 15, 20 and 25 °C; all measurements were done at the optimum water content (i.e. the water content at which the maximal assimilation rate is reached). The radiation source was a KL 2500 LCD (Schott) cold light to avoid heating the samples inside the cuvette. The PPFD response curves were analysed by statistical fitting to a Smith function, as detailed in Green *et al.* (1997), obtaining the following parameters: light compensation point (LCP; the minimal light intensity at which net photosynthesis is reached); PPFDsat (the light intensity at which 90 % of maximal net photosynthesis is reached); and Φ (apparent quantum yield for incident light).

The response of CO_2 exchange to water content was measured as the lichen dried out in flowing air, at a light intensity of 400 μmol photon m^{-2} s^{-1} and 15 °C. The air humidity ranged from 45 to 55 % during the drying experiment for both morphotypes, and the air flow inside the cuvette was 600 mL min^{-1}. The percentage photosynthetic activity was calculated by comparison with the maximum net photosynthesis. Prior to all measurements, samples were soaked in spring water for 20 min to ensure that thalli were fully hydrated. Four replicates of each morphotype for each locality were measured.

Chlorophyll quantification and fluorescence

Chlorophyll was extracted and analysed according to Barnes *et al.* (1992). Absorbance of chlorophyll $a + b$ was measured with an Uvikon XL Spectrophotometer (NorthStar Scientific, UK).

Chlorophyll fluorescence imaging was done with an Imaging-PAM (Walz, Effeltrich, Germany). This method allows the detection of gradients in photosynthetic activation over different parts of the thallus, and the decrease of photosynthetic activity as different parts of the thallus dry out. Thalli were fully hydrated and then allowed to dry out at room temperature and 30 % relative humidity. Short saturation pulses were applied every 15 min to determine the maximum fluorescence yield (F_m') and the fluorescence yield in illuminated samples (F). Effective photosystem II (PSII) quantum yield was then calculated according to Genty *et al.* (1989) as Yield = (F_m' – F)/F_m'. Images obtained were analysed by means of ImageJ free software (National Institutes of Health, Bethesda, MD, USA) to calculate the maximal activity area at the beginning of the experiment and the relative activity area as a percentage of maximal area, as the thalli dried.

Statistical analysis of photosynthetic parameters [analysis of variance (ANOVA) and *t*-tests] was performed with the free software R (R Development Core Team, 2009). Fits to Smith function and graphs were made with SigmaPlot 10·0 (Chicago, IL, USA).

RESULTS

Molecular studies

The samples always rendered clean PCR products, without by-products that would indicate the presence of parasitic fungi, or different algal symbionts in a single thallus.

A total of 679 gene sequences were used in this study, of which 146 were newly generated. Data sets A − H are summarized in Supplementary Data Table S2. The five loci analysed display different levels of genetic variability. Actin is the most variable locus, but indels of different length (1 − 42 bp) account for >20 % of the variable sites. The overall genetic structure of our data set can be deduced from the inferred Bayesian consensus trees for the concatenated mycobiont (Fig. 2A) and photobiont data sets (Fig. 2B). Most of the interior branches of the phylogenies are well supported and generally correspond to geographical sub-groups.

The mycobionts of the Mediterranean populations studied (including the specimens collected in the Spanish *parameras* in this study) are mostly separated by a well-supported branch from the polar populations, but in contrast to Fernández-Mendoza *et al.* (2011) newly sequenced thalli (genotypes 13, 14 and 24 in Fig. 2A) appear intermixed in the polar clades.

The 95 % parsimony probability haplotype networks for the single gene data sets (Fig. 1B, C, D) support the relationships inferred from the concatenated data sets. The dispersion of Mediterranean *C. aculeata* haplotypes among polar and Mediterranean haplotypes is also reflected in the haplotype networks for the separate fungal data sets.

Based on the concatenated fungal data set (F), the nucleotide diversity (π) of vagrant populations is smaller than that of attached populations, regardless of whether sampling locations are pooled or taken separately (Supplementary Data Table S4B, C). This is consistent with the presence of distant genetic lineages in the attached populations that are not present in the vagrant morphs (Fig. 2).

When morphological groups are pooled together, both the exact test of population differentiation and the F_{ST} values suggest that morphological groups form significantly differentiated genetic units, but at the same time show quite low genetic isolation and low values of pairwise genetic distances (D_{xy}; Supplementary Data Table S4B, C). The overall pattern holds when sampling localities are taken into account. It should be noted that the high F_{ST} values estimated between vagrant populations are an artefact due to the extremely low diversity of vagrant populations. Even though the genetic structure of the morphological groups in the hierarchical AMOVAs accounted for approx. 20 % of the total variance of the multilocus and single loci data sets, the differences between vagrant and attached morphs are non-significant (Supplementary Data Tables S4–S6). These results should be interpreted with care as the small sample sizes might bias the results. Finally, permutation tests suggest that vagrant morphs do not represent a random sample of the attached or mixed population, in terms of genetic distances (Supplementary Data Table S6). This result should not be interpreted as evidence of genetic differentiation, but it emphasizes that vagrant morphs are associated with a few closely related multilocus genotypes, which do not represent a sub-set of the global population.

Regarding photobiont diversity and selectivity, our results are consistent with the findings of Fernández-Mendoza *et al.* (2011), and all samples studied (vagrant and attached morphs) belong to strains of *Trebouxia jamesii*. No multilocus genotypes (Fig. 2B) or single gene haplotypes (Fig. 1E, F) are shared between temperate and polar populations for the two photobiont loci after including the newly sequenced vagrant and attached morphs. In the light of genetic data, there are no grounds to support any preferential selectivity between vagrant, attached morphs and the rest of the Mediterranean populations (Supplementary Data Table S4A).

Morphology and anatomy

There is an almost complete gradation between attached morphs of *C. aculeata* and extremely modified thalli in the field observations. However, gradation is not complete in all localities: in Calatañazor, almost no intermediate morphs were found. Attached morphs (Fig. 3A) show an external morphology similar to that described in the literature (e.g. Kärnefelt, 1979). These morphs are usually attached to mosses and to other lichens by thick black strands of fungal hyphae (Fig. 3B, arrow), which resemble the rhizines of some epiphytic lichens. Fixation organs in *Cetraria* had only been previously described for *C. crespoae*.

Intermediate morphs showed a branching pattern similar to that of attached morphs (Fig. 3C), although branches are considerably wider and are clearly foveolate. Excavate pseudocyphellae commonly found in attached morphs expand and become wider and deeper (Fig. 3C). Furthermore, the number of cilia is reduced. Vagrant morphs can display very different morphologies, as can be seen in Fig. 3D and E. In general, the branching system disappears and thalli acquire a more foliose appearance, with very wide lobes, which are generally twisted and show a dorsiventral structure. They also present numerous pits, big holes that seem to have their origin in pseudocyphellae. Although both morphs have pseudocyphellae, they are slightly differerent in their morphology. The attached morphs show excavated and regularly elongated pseudocyphellae, while those of the vagrant morphs are more superficial and irregular in shape (Fig. 3F).

Transversal sections through thalli of attached morphs showed the more or less ellipsoidal shape typical for *C. aculeata* thalli (Fig. 3G). Cortex thickness ranges from 55 to 210 μm (mean 143·7 ± 39·8 μm, $n = 15$). The algal layer is distributed more or less regularly below the cortex layer, although it is possible to observe areas without algal cells (arrows in Fig. 3G), coinciding with the presence of a pseudocyphella. The medulla is lax, with sparse hyphae below the algal layer, usually covered by small calcium oxalate crystals. The central cavity contains very few hyphae.

The cortex of the attached morph is composed of three well differentiated layers (Fig. 3H). Beneath the cortex, it is possible to observe an algal layer, 80 − 190 μm thick (mean 123·9 ± 31·7 μm, $n = 15$), and further below there is a thin medulla with sparsely distributed hyphae, covered with small calcium oxalate crystals. The central part of the thallus is usually hollow.

The structure of transversal sections of vagrant specimens varied among thalli because of their high morphological disparity (Fig. 3D, E). The typical anatomy of vagrant morphs is shown in Fig. 4A. Differences lie in the thickness of the cortex, size of the intercortical space, density of the medulla and degree of development of the lower cortex. The cortex has the same three-layered structure as in attached

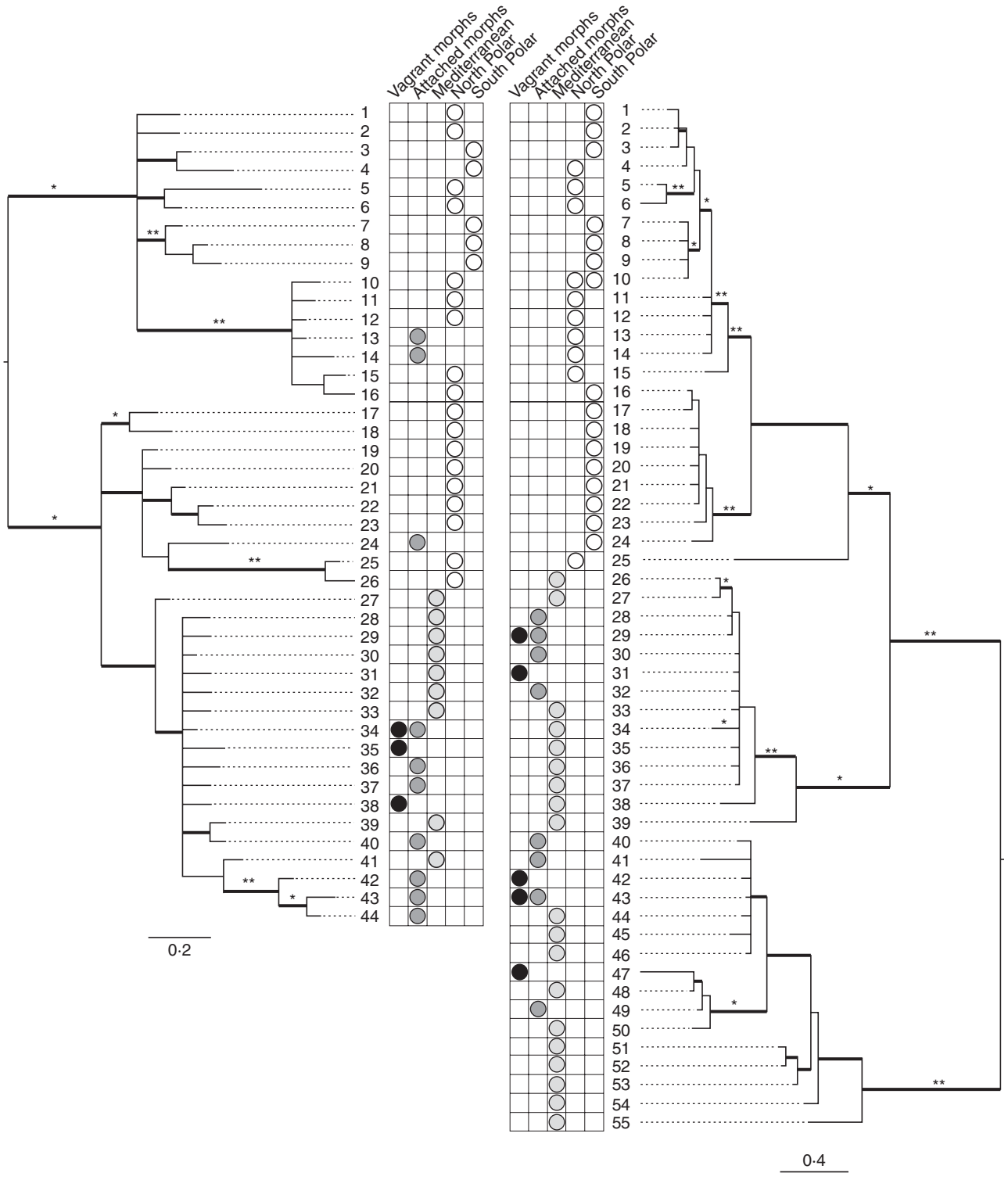

FIG. 2. Unrooted phylogenetic consensus trees of MCMC analyses of the mycobiont data set G (A) and photobiont data set H (B). Shading denotes the geographic origin of the individuals and their sampling scheme: white, polar; light grey, previously sampled Mediterranean *C. aculeata* and *C. steppae*; dark grey, newly collected attached morphs; black, newly collected vagrant morphs. Bold lines indicate posterior probability >0·95.

morphs, although it is considerably thicker (180 − 410 μm; mean 260 ± 62 μm, $n = 15$; *t*-test, $P < 0{\cdot}0001$). Vagrant specimens usually show a dorsiventral thallus structure, with an algal layer only beneath the upper cortex. The presence of a denser algal layer with more algal cells and fungal hyphae is a striking feature in vagrant morphs (Fig. 4A, B). The algal layer is also considerably thicker (130 − 385 μm, mean 262 ± 79·66 μm, *t*-test, $P < 0{\cdot}0001$) and the algal cells have

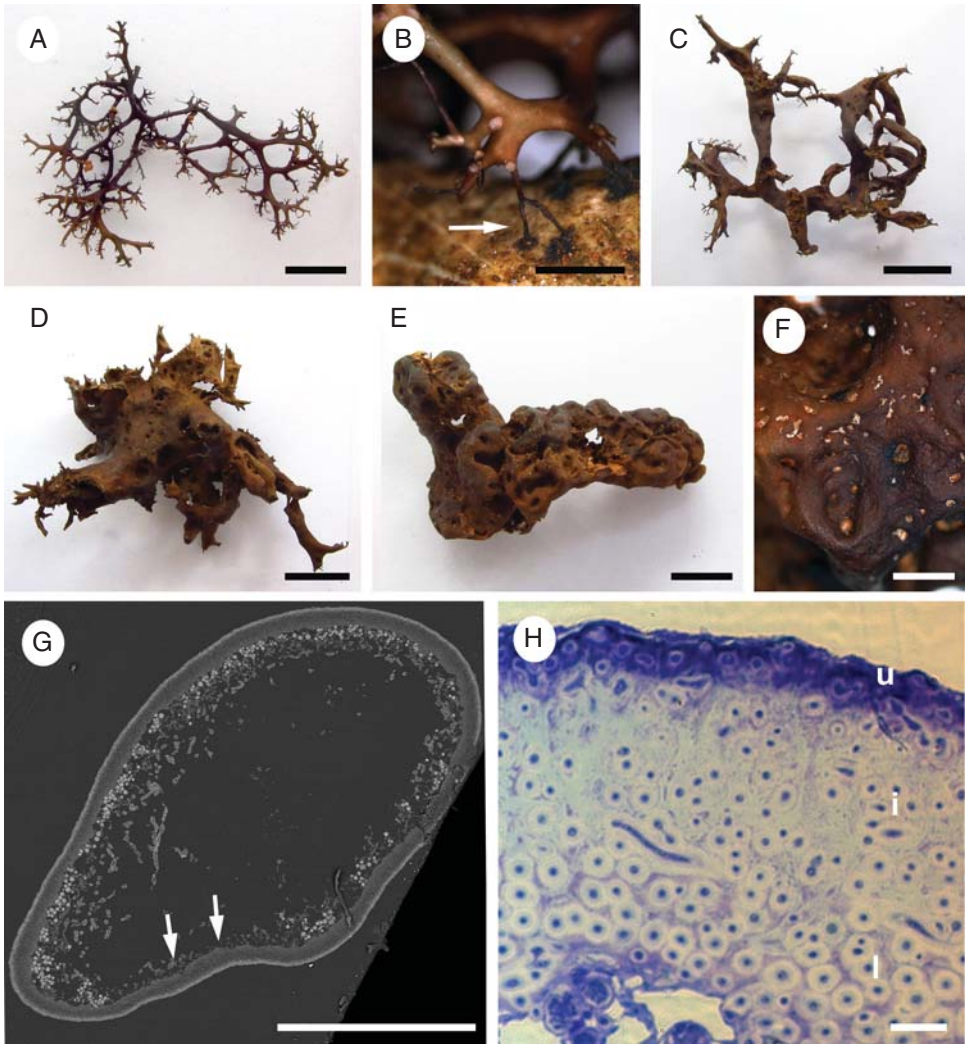

FIG. 3. *Cetraria aculeata*. (A) Attached terricolous thallus (Zaorejas). (B) Detail of rhizines-like structures (arrow) observed in attached thalli from Spanish steppes. The black strands were attached to a *Cladonia convoluta* thallus (Zaorejas). (C) Intermediate morph with wider thallus branches and showing multiple foveae (Iruecha). (D) Vagrant morph with few deformed branches, very wide lobes and numerous holes and foveae (Zaorejas). (E) Vagrant morph showing a globoid shape with a very irregular surface. (F) Detail of the punctiform pseudocyphellae found in the lower surface on vagrant morphs. (G) SEM-BSE photograph of a transversal section of an attached morph; arrows show a thallus area without an algal layer. (H) Light photograph of the three-layered cortex found in attached morphs; a denser methylene blue-stained layer in the upper part with accumulation of dead cells (u), an intermediate layer (i) with hyphae more or less sparsely distributed in a gelatinous matrix with hyphae surrounded by a visible soft stained gel matrix, and a lower layer (l) with more conglutinated fungal cells disposed in a not so evident medium stained gel matrix. Scale bars (A, C–E) = 1 cm; (B, F) = 5 mm; (G) = 200 μm; (H) = 10 μm.

a smaller diameter (mean diameter 9·68 ± 1·79 μm, $n = 1194$) than in attached morphs (mean diameter 11·55 ± 1·68 μm, $n = 200$; *t*-test, $P < 0·0001$). Moreover, the percentage of area occupied by algal cells in the algal layer is statistically different in both morphs, with a mean of 11·90 ± 5·41 % in attached and 17·51 ± 5·06 % in vagrant morphs (*t*-test, $P < 0·001$).

Significant differences in the ultrastructure of algal cells from both morphotypes were not detected (Fig. 4C, D). Algal cells showed the typical *Trebouxia* cell appearance with a large chloroplast containing a central pyrenoid of the *impressa* type (Fig. 4C, D). Pyrenoids from algal cells of vagrant morphs have fewer pyrenoglobuli than those from attached individuals. In attached morphs (Fig. 4C), lipidic storage bodies were slightly more abundant than in vagrant morphs (Fig. 4D).

Vagrant morphs tend to have a denser and more homogeneous medulla (Fig. 4A), although some specimens (e.g. Fig. 3E) showed a central cavity. Medullary fungal hyphae were generally totally covered by calcium oxalate crystals (Fig. 4E, F), which were considerably larger in vagrant (Fig. 4F) than in attached morphs (Fig. 4E), and dispersed in the medullary intercellular spaces (Fig. 4F).

Ultrastructural differences between morph cells were also found in some areas of the cortex. In the inner cortical sub-layer close to the algal layer, attached morphs showed more densely packed fungal hyphae with smaller interhyphal spaces (Fig. 5A)

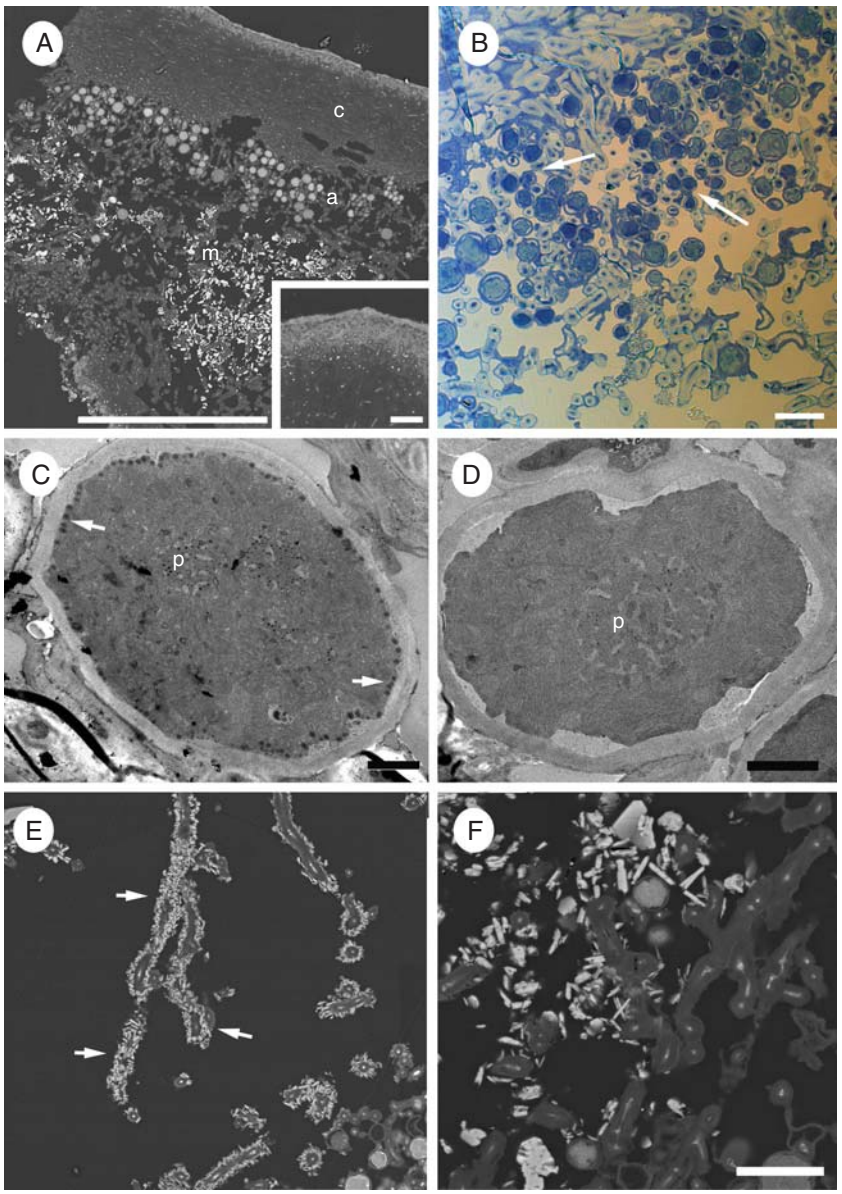

FIG. 4. *Cetraria aculeata*. (A) SEM-BSE photograph of a transversal section of a vagrant morph. The cortex (c) is composed of three layers with a similar structure to that in attached morphs; as can be seen in detail in the inset, the algal layer (a) is only placed below the upper cortex, and the medulla (m) is dense and filled with calcium oxalate crystals. (B) Light photograph of a vagrant morph algal layer; numerous small sized cells are present (arrows). (C) Transmission electron microscopy (TEM) photograph of an algal cell from an attached morph, (p) pyrenoid, (arrows) lipid globules. (D) TEM photograph of an algal cell from a vagrant specimen; letters correspond to the same structures as in (C). (E) SEM-BSE photograph of medullar hyphae from an attached morph, with arrows pointing to calcium oxalate crystals surrounding fungal hyphae. (F) SEM-BSE photograph of medullar hyphae from a vagrant specimen; calcium oxalate crystals are disposed in interhyphal spaces more than surrounding the hyphae. Scale bars: (A) = 200 μm (inset: 20 μm); (B) = 20 μm; (C, D) = 2 μm; (E) = 50 μm; (F) = 20 μm.

than vagrant morphs (Fig. 5B). In vagrant specimens we also observed, in addition to the gelatinous material present in both morphs, fibrous material in the intercellular space that is not directly associated with the hyphal walls (f in Fig. 5B).

Furthermore, the upper cortex of vagrant thalli contained more cells with multilayered cell walls (Fig. 5C), and walls showed more layers (Fig. 5D) than attached thalli. The multilayered cell walls appeared as concentric layers of electron-dense material alternating with electron-transparent layers (Fig. 5D). Additionally, electron-dense layers were also formed by the fibrous material in several thin concentric layers, as can be observed in Fig. 5D.

Chemistry

Norstictic acid was not detected in the samples by means of the microcrystallization technique. The TLC analysis on selected samples only detected lichesterinic and protolichesterinic fatty acids.

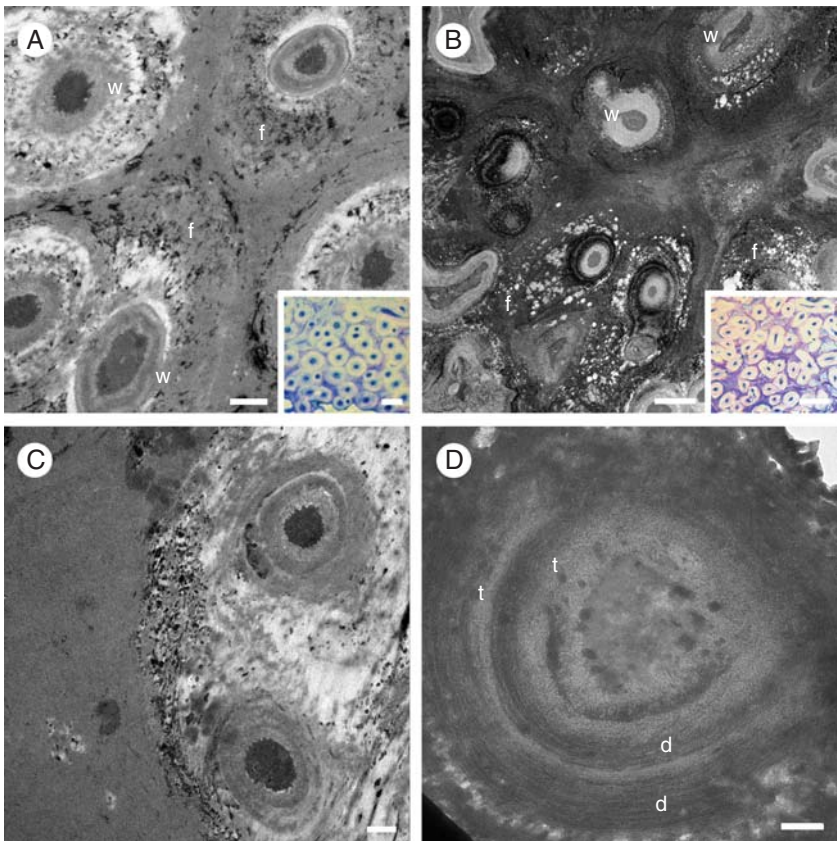

FIG. 5. *Cetraria aculeata*. (A) TEM photograph of the innermost cortical layer of an attached morph (detail of the zone in the light photograph in the inset); fungal cell walls (w) and fibrous matrix (f). (B) TEM photograph of the innermost cortical layer of a vagrant specimen (detail of the zone in the light photograph in the inset); fungal cell walls (w) and fibrous matrix (f). (C) TEM photograph showing two multilayered cell walls embedded in a fibrous matrix from the lower cortical layer of a vagrant specimen. (D) TEM photograph of a multilayered fungal hypha showing concentric layers of electron-dense (d) and electron-transparent material (t). Scale bars: (A) = 1 μm (inset: 5 μm); (B) = 2 μm (square: 5 μm); (C) = 0·5 μm; (D) = 0·2 μm.

Biomass

Total biomass for *C. aculeata* differed among the three localities, with a minimum of $22 \pm 9{\cdot}9$ kg ha^{-1} found in Calatañazor, $32{\cdot}9 \pm 9{\cdot}6$ kg ha^{-1} found in Iruecha and a maximum of $45{\cdot}2 \pm 9{\cdot}6$ kg ha^{-1} found in Zaorejas. The distribution of the biomass was also uneven among morphotypes (Fig. 6). Attached morphs (branch diameter $\leq 1{\cdot}5$ mm) always reached the highest biomass values in the three localities, ranging from $12{\cdot}5 \pm 8{\cdot}8$ kg ha^{-1} in Calatañazor to $17{\cdot}4 \pm 5{\cdot}3$ kg ha^{-1} in Zaorejas. Intermediate vagrant morphs ($1{\cdot}5$ mm $<$ branch diameter ≤ 3 mm) showed intermediate values (but not in Zaorejas where they represented the group with the lowest biomass). Vagrant morphs (branch diameter $>$ 3 mm) varied greatly from one locality to another, not only in absolute biomass but also as a percentage of the total *C. aculeata* biomass in the locality. In Calatañazor, for instance, vagrant morphs reached $3 \pm 2{\cdot}4$ kg ha^{-1} or 13·8 % of the total biomass of *C. aculeta*. In contrast, vagrant morphs in Zaorejas reached $16{\cdot}6 \pm 6{\cdot}4$ kg ha^{-1}, 36·8 % of the total biomass in that locality.

Water content, gas exchange and chlorophyll fluorescence

Photosynthesis was measured for 24 thalli, 12 replicates per morphotype. The grouping of individual thalli into morphotypic groups is supported by the lack of significant differences in performance between localities within morphotypes (data not shown).

Overall the two morphotypes show very few significant differences in their photosynthetic response to temperature and light. The photosynthetic response curves (Fig. 7) for both morphotypes were very similar at temperatures ranging between 5 and 25 °C. Moreover, no significant differences were found in dark respiration and A_{max} (Supplementary Data Table S7), despite the consistently higher values for attached thalli. The parameters obtained by Smith function fitting of light curves: LCP, PPFDsat and Φ (Green *et al.*, 1997) (Supplementary Data Table S7), only differed significantly ($P < 0{\cdot}05$) between the morphotypes for LCP at 5 °C and PPFDsat at 15 °C. All other parameters suggest that photosynthetic response to light does not differ between morphotypes. Chlorophyll content did not differ significantly either, with average values of $0{\cdot}6 \pm 0{\cdot}12$ mg g d. wt^{-1} for attached thalli and $0{\cdot}57 \pm 0{\cdot}14$ mg g d. wt^{-1} for vagrant morphs ($\pm$ SD, $n = 12$).

In contrast to their similar response to light and temperature conditions, both morphs showed marked differences in water-holding capacity and desiccation dynamics. Water-holding capacity is significantly higher (P-value $<0{\cdot}001$) in vagrant morphs, which held $247{\cdot}6 \pm 25{\cdot}58$ % of d. wt, compared

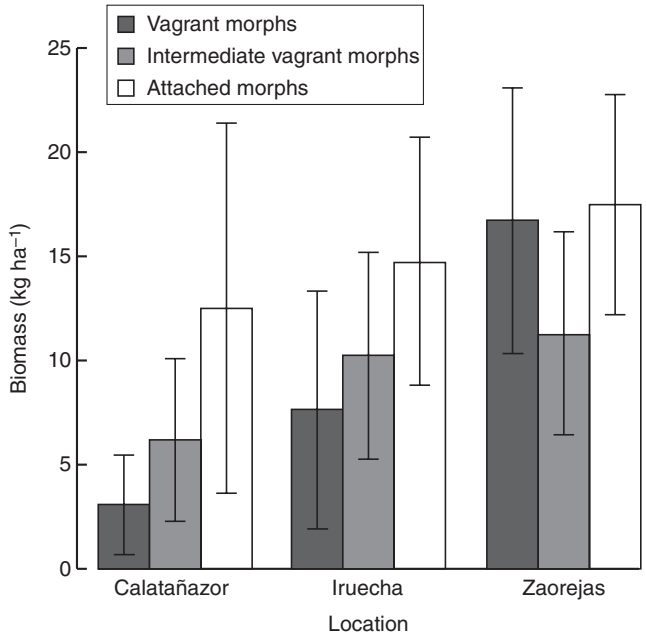

FIG. 6. Biomass of *Cetraria aculeata* from the three localities sampled in this study. 'Vagrant morphs', specimens > 3 mm; 'intermediate vagrant morphs', 1·5 mm < specimens ≤ 3 mm; 'attached morphs', specimens with maximum branch diameter ≤ 1·5 mm. Error bars show the 95 % normal confidence intervals used in the text.

with attached morphs, with 223·6 ± 27·02 % of water in dry mass.

The morphotypes also differed in their dynamics of physiological activity during desiccation. The water curves of Fig. 8E show the percentage of activity during desiccation for both morphotypes, at 15 °C and 400 μmol photon m^{-2} s^{-1}. Attached thalli dried much faster than vagrant morphs (Fig. 8E), in spite of the differences found within groups. The latter have a much longer period of physiological activity, maintaining greater net photosynthesis for about 3 h longer than the attached thalli.

Water retention and physiological activity were also studied by means of chlorophyll fluorescence (Fig. 8A–D). Images taken at the beginning of drying with fully hydrated thalli and after 45 min into the desiccation gradient showed very different patterns for both morphs. Attached thalli dried quite quickly, showing no fluorescence yield after 45 min. Vagrant morphs on the other hand maintained 44 % of their active area after 45 min.

DISCUSSION

We describe here an extreme case of phenotypic variation (Bradshaw, 1965; Valladares *et al.*, 2007) in the terricolous, cosmopolitan species *C. aculeata*. In steppe areas of Central Spain, vagrant specimens display an exceptional morphology that deviates from their typical fruticose thalli with more or less terete branches. This phenomenon is not unique, and similar modifications for this species have been observed in other steppe areas of Iran and Ukraine (M. Sohrabi and O. Nadyeina, pers. comm.).

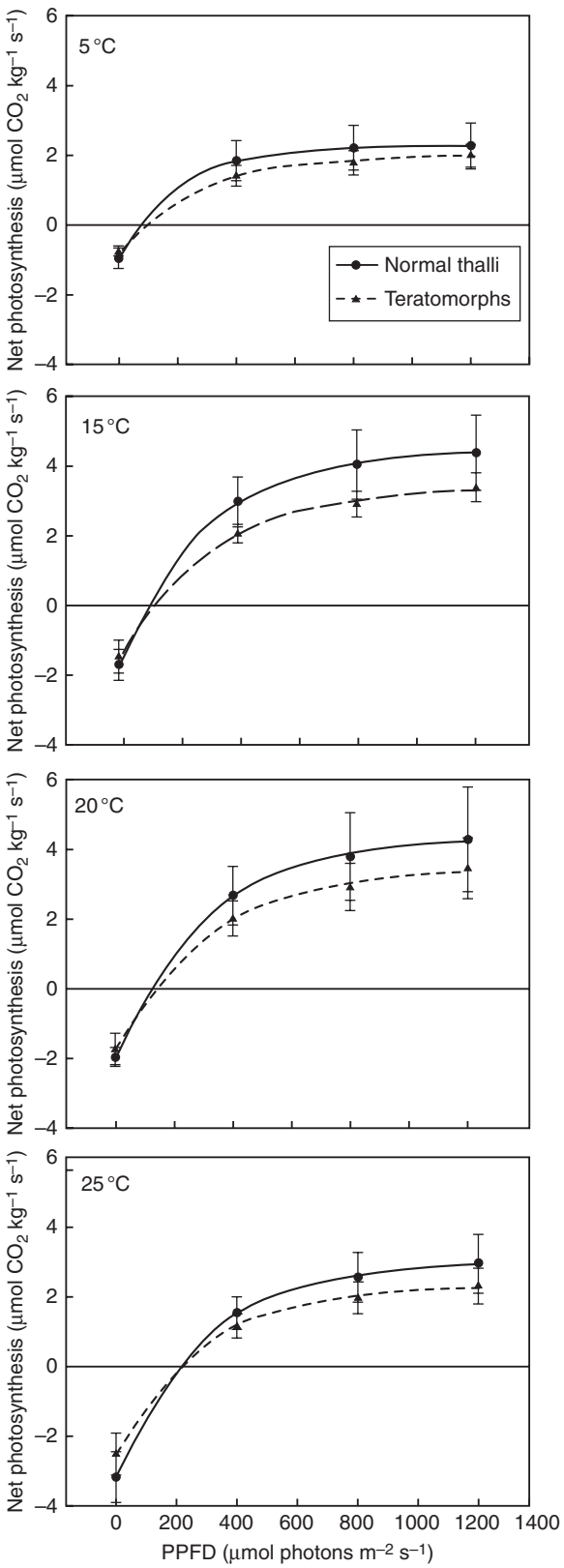

FIG. 7. Photosynthetic performance of morphs of *Cetraria aculeata* under controlled conditions of irradiation and temperature in the laboratory. Measurements were made at optimum water content.

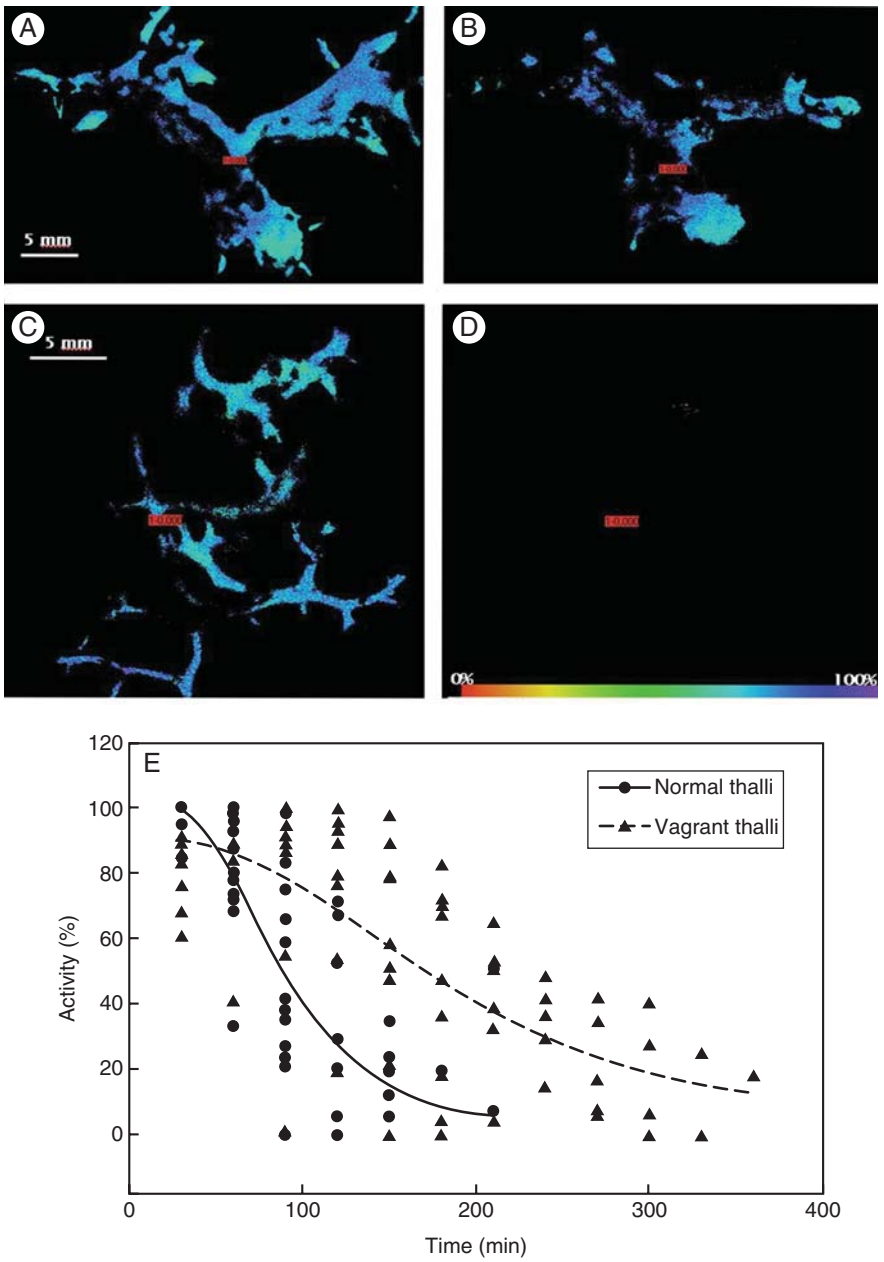

FIG. 8. (A–D) Fluorescence imaging captions of both morphotypes during air drying. (A, B) Vagrant morphs at 0 and 45 min. (C, D) Attached morphs at 0 and 45 min. The scale shows the percentage of PSII fluorescence yield. (E) Drying curves under laboratory controlled conditions (see text), showing time course of net photosynthetic activity for both morphs.

Extreme modifications present in the vagrant forms of *C. aculeata* in these habitats lead to confusion regarding its taxonomy and phylogenetic affinity. We show that the vagrant specimens sampled for this study belong to the *C. aculeata* clade as identified in Fernández-Mendoza *et al.* (2011). They do not form a separate phylogenetic group, but they lie within the same clade as the core of Mediterranean samples in the concatenated phylogeny (Fig. 2A), which also includes *C. steppae*, a taxon that requires a further revision and that had been confused with the vagrant morphs. Thus, the genetic support for the occurrence of *C. steppae* in Spain is weak. The vagrant morphs from Central Spain do not share any haplotypes with the specimens identifiable as *C. steppae*. A similar delimitation problem also exists with *C. aculeata* and the very similar *C. muricata* (Kärnefelt *et al.*, 1993; Thell *et al.*, 2000, 2002). We have not sampled thalli that could morphologically be identified as *C. muricata*. Our phylogenetic reconstruction includes inconsistencies which affect a very limited number of combined haplotypes (13, 14 and 24 in Fig. 2A) in which sequences assigned to distant ITS and GPD clades are shuffled. The presence of distant lineages in ITS gives an *a priori* impression that the attached populations are formed by two genetically isolated units, but this idea does not hold when other

markers are taken into account. These divergent ITS haplotypes are associated with the attached morphs and in fact contribute to the magnitude of the differentiation estimates between both morphs. Based on our current data, it seems sensible to understand this as part of the polymorphism of the populations, overlooking its origin, but it highlights the need to address genealogical lineage sorting and gene flow between lineages when dealing further with phylogeographic and species delimitation studies.

A second question addresses whether vagrant and attached morphs form actually separate genetic units. In the single gene data sets, vagrant and typical morphs of *C. aculeata* share haplotypes with each other, and only one ITS haplotype and two GPD haplotypes are exclusive to the vagrant morph (Fig. 1B, D). Genetic diversity of non-vagrant sub-populations is higher (Supplementary Data Table S4B, C) than that of the vagrant populations. In that respect, even though no private genotypes were found, the vagrant morph is associated with few closely related haplotypes (Fig 1B, C, D). Permutation tests suggest that vagrant thalli do not correspond to a random sample taken from the mixed or attached population, which would be expected if stochastic processes such as viral or fungal infections or simply random detachment from the substrate were responsible for the deviating morphology.

Results based on the current genetic data show two contrasting patterns, as the tests of population differentiation and the permutation tests show significant differences while the estimates of genetic differentiation (D_{xy}) and isolation (F_{ST}) are low, and the AMOVAs are not significant. (Supplementary Data Table S4B, C). As a whole, these results suggest that even though vagrant morphs do not constitute a separate evolutionary entity, and the vagrant morphotype might be acquired after detaching from the substrate, the development of a new anatomical pattern only happens in a particular group of closely related genotypes, suggesting the presence of a differentiated genetic group.

A genetic basis for local adaptation has been shown in numerous plants, animals and fungi (e.g. Byars *et al.*, 2009; Bongaerts *et al.*, 2010; Mueller *et al.*, 2011). However, no study has so far focused on the genetic basis of local adaptations in lichenized fungi. Our data suggest that the extreme phenotypic variation found in *C. aculeata* in steppe habitats might have a genetic basis, and that some genotypes could have been locally selected under the particular environmental conditions. Our results conform with those of Leavitt *et al.* (2011*c*), who found that some lineages of the saxicolous lichen species *Rhizoplaca melanophtalma* may have an underlying genetic predisposition to vagrancy. Likewise, Leavitt *et al.* (2011*a*, *b*) found that some lineages of the saxicolous foliose genus *Xanthoparmelia* comprised both saxicolous and vagrant specimens.

Photobionts in both *C. aculeata* morphs were identified as *T. jamesii*, which is consistent with previous results for the species (Fernández-Mendoza *et al.*, 2011). Both morphs do not differ in their photobiont selectivity, as vagrant and attached morphs share the same algal multilocus genotypes. Those fungal genotypes found which appeared intermixed within the polar clades (Figs. 1B, C, D and 2A) also share the same Mediterranean algal strains, supporting the idea that photobiont use is strongly modulated by climate (Fernández-Mendoza *et al.*, 2011).

The striking morphological changes displayed in vagrant *C. aculeata* morphs have an anatomical and ultrastructural basis. Vagrant specimens acquire a dorsiventral thallus structure, with an algal layer only beneath the upper cortex layer. Cortical and algal layers become thicker, and the medulla is filled by a denser hyphal network interspersed with large calcium oxalate crystals. Morphological variation in lichen species as an adaptation to different environments or microhabitats has been shown for many species (Larson *et al.*, 1986; Nash *et al.*, 1990; Pintado *et al.*, 1997; Rikkinen, 1997; Sojo *et al.*, 1997). Such morphological adaptations to different environments have usually been interpreted as different strategies in water uptake and retention (Larson and Kershaw, 1976; Larson, 1981; Rundel, 1982; Fos *et al.*, 1999). Pintado *et al.* (1997) found that in fruticose lichens the influence of thallus size and shape on water retention is greater than the role of thallus anatomy. However, this is not necessarily true for other lichen biotypes such as foliose species (Valladares *et al.*, 1998). In our study, vagrant morphs tend to acquire morphologies with a lower surface to volume ratio (Fig. 3A–E), which leads to higher water storage capacities and decreased water loss by evaporation (Larson and Kershaw, 1976; Rundel, 1982; Sancho *et al.*, 2000). This fact, confirmed by the longer period of photosynthetic activity measured for vagrant morphs, corroborates the great influence of morphology on the water relations in fruticose lichens.

The thicker cortex and denser medullary layer shown by vagrant forms seem to be related to thallus water relations. A relationship between increased thickness of cortical layers and higher light intensities was postulated by Grube (2010), but we have not found consistent differences in light responses between the morphs (Fig. 7). Differences in water uptake and water loss were also related to lichen anatomy (Sancho and Kappen, 1989; Valladares *et al.*, 1993), and cortical and medullary structures may be of crucial importance for water relations in lichen thalli (Snelgar and Green, 1981; Rundel, 1982). However, in the foliose lichen family Umbilicariaceae, a direct relationship between cortex thicknesses or medullary structure and a higher water storage capacity was not found (Valladares, 1994; Valladares *et al.*, 1994). Likewise, Pintado *et al.* (1997) found no correlation between two anatomically different ecotypes of the saxicolous *Ramalina capitata* var. *protecta* growing in opposite faces of the same rock and their hydric properties. In *C. aculeata*, the thicker cortex and denser medullary layer in vagrant morphs are likely to be related to their greater capacity (longer retention times) for water storage, although it is difficult to differentiate the role of thallus size and shape and thallus anatomy in the hydric properties.

The smaller algal cells found in vagrant morphs may be related to undergoing rapid cell division, which usually occurs in younger parts of a thallus such as lobe apices (Anglesea *et al.*, 1983; Hill, 1989, 1994). In contrast, in attached morphs, most of the cells are large, probably surpassing the maximum cell size for division (Hill, 1989, 1992). The presence of algal cells within the medullary layer in vagrant morphs (Fig. 4A) could indicate that algal cells are

redistributed from one side to the other as the thallus becomes dorsiventral (Jahns, 1970).

The presence of larger calcium oxalate crystals in the medulla of vagrant morphs may be interpreted depending on different roles in lichen biology that were attributed to this substance. In other vagrant lichens such as *Xanthoparmelia convoluta*, increased rigidity and strength of the thallus has been attributed to calcium oxalate deposits in the medulla (Modenesi *et al.*, 2000). A different functional role as radiation reflectors has been recognized for calcium oxalate crystals (Kappen, 1988; Modenesi *et al.*, 2000). The increased accumulation of these crystals and their larger size in vagrant morphs could thus be related to the enlargement of the cortex and a reduction of the light available for algae. Likewise, the presence of a small number of pyrenoglobuli and the lack of lipid bodies in the algal cytoplasm of the vagrant morphs can be interpreted as an adaptation to lower light intensities (Brown *et al.*, 1988).

The multilayered walls in cortical hyphae found in vagrant morphs point to the presence of diffuse growth. The continuous production of cell wall layers producing a multilayered structure has previously been observed in *Ramalina menziesii* (Sanders and Ascaso, 1995) where it was related to diffuse growth (=intercalary growth, see Sanders 2001) and to the way in which fungal hyphae retain their integrity when cell elongation occurs. Although most lichen species are thought to grow apically (Anglesea *et al.*, 1983; Greenhalgh and Whitfield, 1987), diffuse growth has been reported for several species (Sanders and Ascaso, 1995; Rolstad and Rolstad, 2008; Voisey, 2011) and it might be more common than previously thought (Honegger, 2008). This diffuse growth may facilitate the morphological changes detected in vagrant morphs of *C. aculeata* (Sanders and Ascaso, 1995).

The stunning changes in thallus shape and anatomy observed in vagrant specimens from steppe areas raise the question of what factor triggers the beginning of the changes that culminate in deformed thalli. It seems clear that the presence of deformations is linked to the vagrant habit as such morphs have only been reported from steppe areas where the presence of vagrant lichens is common. Vagrancy is apparently related to the special environmental conditions present in those habitats (wind-swept desert or semi-desert areas).

Cetraria aculeata probably has a basal–apical thallus polarity, where growth is associated with apical pseudomeristematic areas as also known from other terricolous species (Hammer, 2000). The processes and factors ruling this polarity are so far unknown. When *C. aculeata* detaches from soil in steppe areas, probably due to solifluxion phenomena and wind, the basal–apical polarity would disappear, or, due to the flattening suffered by the thalli, the point-like apical growth zone could become a line-like marginal growth zone. These possibilities might trigger diffuse growth processes in different parts of the thallus because the loss of a unique apical dominance would lead to a disordered growth of hyphae (Weber, 1977; Harris, 2010). Responses to spatial disturbances have been studied in few lichen species (Honegger, 1995, 1996). Honegger (1996) studied the responses of two species of lichens − *Xanthoria parietina* and *Parmelia sulcata* − subjected to spatial disturbances, observing that thalli corrected spatial disturbances trying to secure adequate illumination for the photobiont population. She concluded that species are 'capable of sensing, in a manner yet unknown, spatial disturbances and partly correcting them by means of growth processes' (Honegger, 1996). The phenomenon has also been observed in the field in species of *Peltigera* and *Cladonia*, and seems to be related to light rather than gravity (Nienburg, 1919; von Goebel, 1926; Jahns, 1970; Honegger, 1996).

Finally, the longer period of activity in vagrant morphs, due to their greater water retention capacity, allows them a higher carbon gain which could facilitate higher growth rates of the mycobiont. The thicker cortex and lower surface to volume ratio could also provide protection against mechanical damage, taking into account that vagrant morphs usually live in less sheltered habitats than attached morphs.

To conclude: the morphological and anatomical changes shown by the vagrant morphs of *C. aculeata* from steppe regions in Central Spain represent one of the most extreme cases of infraspecific phenotypic variation found in lichens. These changes can be interpreted in different ways. They could be the result of spatial disturbances after thalli have become vagrant without any evolutionary relevance. The loss of the basal–apical axis polarity could result in changes of growth patterns, with diffuse growth probably displacing apical growth, as witnessed by the common presence of multilayered cell walls in vagrant morphs. However, the genetic and ecophysiological data indicated a genetic and hence adaptational background of the changes, although this seems not to have led to speciation. More accurate markers (e.g. microsatellites) should be used to test the hypothesis of genetic isolation between populations of the two morphs. The higher water storage capacity and ensuing longer periods of photosynthetic activity could be interpreted as an adaptation to the drier climatic conditions in the *parameras* of Central Spain. This hypothesis of enhanced fitness is supported by the greater biomass of vagrant morphs found in all localities. Our results and recently published studies (Leavitt *et al.*, 2011*a*, *b*, *c*) suggest that substantial morphological variation is more common in lichens than previously thought.

SUPPLEMENTARY DATA

Supplementary data are available online at www.aob.oxfordjournals.org and consist of the following tables. Table S1: sampling localities used in the study. Table S2: summary statistics, PCR setting and substitution models for data sets used in the study. Table S3: structure of the fungal and algal data sets. Table S4: pairwise estimates of gene flow and differentiation between morphological groups stratified by sampling localities based on the concatenated three-loci data set for the mycobiont and the two-loci data set for the photobiont. Table S5: results of the AMOVA analysis and the tests for population differentiation on the concatenated and single loci data sets implemented in Arlequin v 3·5. Table S6: results of the permutation tests based on JC69 genetic distances using all collected thalli and only non-teratomorphic thali as sources for the null distribution. Table S7: photosynthetic data.

ACKNOWLEDGEMENTS

We thank W. Sanders (Florida Gulf Coast Univeristy) and two anonymous referees for their helpful comments on earlier versions of the article. This study was partially funded by the project CTM2009-12838-C04-03/ANT (Ministerio de Ciencia e Innovación, Spain), by the research funding programme 'LOEWE–Landes-Offensive zur Entwicklung Wissenschaftlich-ökonomischer Exzellenz' of Hesse's Ministry of Higher Education, Research, and the Arts, and by the German Science Foundation (DFG-grant Pr 567/13-1). S.P.O. is grateful to the JAE-Doc program (CSIC, Spain) for support. Heike Kappes, Selina Becker and Maike Fibian are thanked for technical support in the lab.

LITERATURE CITED

Anglesea D, Greenhalgh GN, Veltkamp CJ. 1983. The structure of the thallus tip in *Usnea subfloridana*. *Lichenologist* **15**: 73–80.

Barnes JD, Balaguer L, Manrique E, Elvira S, Davison AW. 1992. A reappraisal of the use of DMSO for the extraction and determination of chlorophyll a and b in lichens and higher plants. *Environmental and Experimental Botany* **32**: 85–100.

Bongaerts P, Riginos C, Ridgway T, *et al*. 2010. Genetic divergence across habitats in the widespread coral *Seriatopora hystrix* and its associated *Symbiodinium*. *PLoS ONE* **5**: e10871. http://dx.doi:10.1371/journal.pone.0010871.

Bradshaw AD. 1965. Evolutionary significance of phenotypic plasticity in plants. *Advances in Genetics* **13**: 115–155.

Brown DH, Ascaso C, Rapsch S. 1988. Effects of light and dark on the ultrastructure of lichen algae. *Annals of Botany* **62**: 625–632.

Büdel B, Wessels DCJ. 1986. *Parmelia hueana* Gyeln., a vagrant lichen from the Namib Desert, SWA/Namibia. I Anatomical and reproductive adaptations. *Dinteria* **18**: 3–12.

Byars SG, Parsons Y, Hoffmann AA. 2009. Effect of altitude on the genetic structure of an Alpine grass, *Poa hiemata*. *Annals of Botany* **103**: 885–899.

Clement M, Posada D, Crandall KA. 2000. TCS: a computer program to estimate gene genealogies. *Molecular Ecology* **9**: 1657–1660.

Crespo A, Barreno E. 1978. Sobre las comunidades terricolas de liquenes vagantes (*Sphaerothallio-Xanthoparmelion vagantis* al. nov.). *Acta Botanica Malacitana* **4**: 55–62.

Drummond AJ, Ashton B, Buxton S, *et al*. 2010. *Geneious v5·3*. Available from http://www.geneious.com/.

Edgar R. 2004. MUSCLE: a multiple sequence alignment method with reduced time and space complexity. *BMC Bioinformatics* **5**: 113. http://dx.doi:10.1186/1471-2105-5-113.

Eldridge DJ, Leys JF. 1999. Wind dispersal of the vagrant lichen *Chondropsis semiviridis* in semi-arid eastern Australia. *Australian Journal of Botany* **47**: 157–164.

Elenkin A. 1901. Les Lichens migrateurs. *Bulletin du Jardin Imperiale Botanique de Saint* Pétersbourg **1901**: 16–38, 52–72.

Excoffier L, Smouse P, Quattro J. 1992. Analysis of molecular variance inferred from metric distances among DNA haplotypes: application to human mitochondrial DNA restriction data. *Genetics* **131**: 479–491.

Excoffier L, Lischer HEL. 2010. Arlequin suite ver 3·5: a new series of programs to perform population genetics analyses under Linux and Windows. *Molecular Ecology Resources* **10**: 564–567.

Fernández-Mendoza F, Domaschke S, García MA, Jordan P, Martín MP, Printzen C. 2011. Population structure of mycobionts and photobionts of the widespread lichen *Cetraria aculeata*. *Molecular Ecology* **20**: 1208–1232.

Fos S, Deltoro VI, Calatayud A, Barreno E. 1999. Changes in water economy in relation to anatomical and morphological characteristics during thallus development in *Parmelia acetabulum*. *Lichenologist* **31**: 375–387.

Genty B, Briantais JM, Baker NR. 1989. The relationship between the quantum yield of photosynthetic electron transport and quenching of chlorophyll fluorescence. *Biochimica et Biophysica Acta* **990**: 87–92.

von Goebel K. 1926. Morphologische und biologische Bemerkungen. 32. *Induzierte Dorsiventralität bei Flechten* **121**: 177–188.

Green TGA, Büdel B, Meyer A, Zellner H, Lange OL. 1997. Temperate rainforest lichens in New Zealand: light response of photosynthesis. *New Zealand Journal of Botany* **35**: 493–504.

Greenhalgh GN, Whitfield A. 1987. Thallus tip structure and matrix development in *Bryoria fuscescens*. *Lichenologist* **19**: 295–305.

Grube M. 2010. Die hard: lichens. In: Seckbach J, Grube M. eds. *Symbioses and stress: joint ventures in biology (Cellular origin, life in extreme habitats and astrobiology)*. Vol. 17. Dordrecht: Springer, 509–523.

Hammer S. 2000. Meristem growth dynamics and branching patterns in the Cladoniaceae. *American Journal of Botany* **87**: 33–47.

Harris SD. 2010. Hyphal growth and polarity. In: Borkovich KA, Ebbole DJ. eds. *Cellular and molecular biology of filamentous fungi*. Washington, DC: ASM Press, 238–259.

Hill DJ. 1989. The control of the cell cycle in microbial symbionts. *New Phytologist* **112**: 175–184.

Hill DJ. 1992. Lobe growth in lichen thalli. *Symbiosis* **12**: 43–55.

Hill DJ. 1994. The cell cycle of the photobiont of the lichen *Parmelia sulcata* (Lecanorales, Ascomycotina) during development of the thallus lobes. *Cryptogamic Botany* **4**: 270–273.

Honegger R. 1995. Experimental studies with foliose macrolichens: fungal responses to spatial disturbance at the organismic level and to spatial problems at the cellular level during drought stress events. *Canadian Journal of Botany* **73**: 569–578.

Honegger R. 1996. Experimental studies of growth and regenerative capacity in the foliose lichen *Xanthoria parietina*. *New Phytologist* **133**: 573–581.

Honegger R. 2008. Morphogenesis. In: Nash TH III. ed. *Lichen biology*, 2nd ed. Cambridge: Cambridge University Press, 69–93.

Jackson HB, St.Clair LL, Eggett DL. 2006. Size is not a reliable measure of sexual fecundity in two species of lichenized fungi. *Bryologist* **109**: 157–165.

Jahns HM. 1970. Untersuchungen zur Entwicklungsgeschichte der Cladoniaceen mit besonderer Berucksischtigung des Podetien–Problems. *Nova Hedwigia* **20**: 1–177.

Jukes TH, Cantor CR. 1969. Evolution of protein molecules. In: Munro HN. ed. *Mammalian protein metabolism*. New York: Academic Press, 21–123.

Kappen L. 1982. Lichen oases in hot and cold deserts. *Journal of the Hattori Botanical Laboratory* **53**: 325–330.

Kappen L. 1988. Ecophysiological relationships in different climatic regions. In: Galun M. ed. *CRC handbook of lichenology*, Vol. II. Boca Raton, FL: CRC Press, 37–100.

Kappen L. 2000. Some aspects of the great success of lichens in Antarctica. *Antarctic Science* **12**: 314–324.

Kärnefelt I, Mattsson JE, Thell A. 1993. The lichen genera *Arctocetraria, Cetraria*, and *Cetrariella* (Parmeliaceae) and their presumed evolutionary affinities. *Bryologist* **96**: 394–404.

Kärnefelt I. 1979. The brown fruticose species of *Cetraria*. *Opera Botanica* **46**: 1–150.

Kärnefelt I. 1986. The genera *Bryocaulon*, *Coelocaulon* and *Cornicularia* and formerly associated taxa. *Opera Botanica* **86**: 1–90.

Kunkel G. 1980. Microhabitat and structural variation in the *Aspicilia desertorum* group (lichenized Ascomycetes). *American Journal of Botany* **67**: 1137–1144.

Lange OL, Green TGA, Meyer A, Zellner H. 2008. Epilithic lichens in the Namib fog desert; field measurements of water relations and carbon dioxide exchange. *Sauteria* **15**: 283–302.

Larson DW. 1981. Differential wetting in some lichens and mosses: the role of morphology. *Bryologist* **84**: 1–15.

Larson DW. 1989. Differential heat sensitivity amongst four populations of the lichen *Ramalina menziesii* Tayl. *New Phytologist* **111**: 73–79.

Larson DW, Kershaw KA. 1976. Studies on lichen-dominated systems. XVIII. Morphological control of evaporation in lichens. *Canadian Journal of Botany* **54**: 2061–2073.

Larson DW, Matthes-Sears U, Nash THIII. 1986. The ecology of *Ramalina menziesii*. I. Geographical variation in form. *Canadian Journal of Botany* **63**: 2062–2068.

Leavitt SD, Johnson LA, Goward T, St.Clair LL. 2011*a*. Species delimitation in taxonomically difficult lichen-forming fungi: an example from morphologically and chemically diverse *Xanthoparmelia* (Parmeliaceae) in North America. *Molecular Phylogenetics and Evolution* **60**: 317–332.

Leavitt SD, Johnson LA, St.Clair LL. 2011*b*. Species delimitation and evolution in morphologically and chemically diverse communities of the lichen-forming genus *Xanthoparmelia* (Parmeliaceae, Ascomycota) in western North America. *American Journal of Botany* **98**: 175–188.

Leavitt SD, Fankhauser JD, Leavitt DH, Porter LD, Johnson LA, St.Clair LL. 2011*c*. Complex patterns of speciation in cosmopolitan 'rock posy' lichens – discovering and delimiting cryptic fungal species in the lichen–forming *Rhizoplaca melanophthalma* species-complex (Lecanoraceae, Ascomycota). *Molecular Phylogenetics and Evolution* **59**: 587–602.

Librado P, Rozas J. 2009. DnaSP v5: a software for comprehensive analysis of DNA polymorphism data. *Bioinformatics* **25**: 1451–1452.

Lumbsch HT, Kothe HW. 1988. Anatomical features of *Chondropsis semiviridis* (Nyl.) Nyl. in relation to its vagrant habit. *Lichenologist* **20**: 25–29.

Lynch M, Crease TJ. 1990. The analysis of population survey data on DNA sequence variation. *Molecular Biology and Evolution* **7**: 377–394.

Modenesi P, Piana M, Giordani P, Tafanelli A, Bartoli A. 2000. Calcium oxalate and medullary architecture in *Xanthomaculina convoluta*. *Lichenologist* **32**: 505–512.

Mueller UG, Mikheyev AS, Hong E, *et al*. 2011. Evolution of cold-tolerant fungal symbionts permits winter fungiculture by leafcutter ants at the northern frontier of a tropical ant–fungus symbiosis. *Proceedings of the National Academy of Sciences, USA* **108**: 4053–4056.

Nash THIII, Boucher VL, Gebauer R, Larson DW. 1990. Morphological and physiological plasticity in *Ramalina menziesii*: studies with reciprocal transplants between a coastal and inland site. *Bibliotheca Lichenologica* **38**: 357–365.

Nei M. 1987. *Molecular evolutionary genetics*. New York: Columbia University Press.

Nienburg W. 1919. Studien zur Biologie der Flechten, III. Transversalphototropismus bei Flechten. *Zeitschrift fur Botanik* **11**: 1–38.

Nylander JAA, Wilgenbusch JC, Warren DL, Swofford DL. 2004. AWTY (are we there yet?): a system for graphical exploration of MCMC convergence in Bayesian phylogenetics. *Bioinformatics* **24**: 581–583.

Orange A, James PW, White FJ. 2001. *Microchemical methods for the identification of lichens*. London: British Lichen Society.

Paradis E, Claude J, Strimmer K. 2004. *APE*: analyses of phylogenetics and evolution in R language. *Bioinformatics* **20**: 289–290.

Paradis P. 2010. Pegas: an R package for population genetics with an integrated modular approach. *Bioinformatics* **26**: 419–420.

Pérez FL. 1997. Geoecology of erratic lichens of *Xanthoparmelia vagans* in an equatorial Andean paramo. *Plant Ecology* **129**: 11–28.

Pintado A, Valladares F, Sancho LG. 1997. Exploring phenotypic plasticity in the lichen *Ramalina capitata*: morphology, water relations and chlorophyll content in north- and south-facing populations. *Annals of Botany* **80**: 345–353.

Plusnin SN. 2004. Morphological adaptation of the lichen *Stereocaulon alpinum* (Stereocaulaceae) in tundra ecosystems. *Botanicheskii Zhurnal* **89**: 1437–1452.

Posada D. 2008. jModelTest: phylogenetic model averaging. *Molecular Biology and Evolution* **25**: 1253–1256.

R Development Core Team. 2009. *R: a language and environment for statistical computing*. http://www.R-project.org.

Rambaut A, Drummond AJ. 2010. *Tracer v1·5*. Available from http://beast.bio.ed.ac.uk/Tracer

Raymond M, Rousset F. 1995. An exact test for population differentiation. *Evolution* **49**: 1280–1283.

Reynolds S. 1963. The use of lead citrate at high pH as an electron-opaque stain in electron microscopy. *Journal of Cell Biology* **17**: 200–211.

Rikkinen J. 1997. Habitat shifts and morphological variation of *Pseudevernia furfuracea* along a topographical gradient. *Symbolae Botanicae Upsalienses* **32**: 223–245.

de los Ríos A, Ascaso C. 2002. Preparative techniques for transmission electron microscopy and confocal laser scanning microscopy of lichens. In: Cramer I, Beckett RP, Varma KK. eds. *Protocols in lichenology*. Berlin: Springer-Verlag, 87–117.

Rivas-Martínez S, Díaz TE, Fernández-González F, *et al*. 2002. Vascular plant communities of Spain and Portugal. Addenda to the syntaxonomical checklist of 2001. *Itinera Geobotanica* **15**: 5–922.

Rolstad J, Rolstad E. 2008. Intercalary growth causes geometric length expansion in Methuselah's beard lichen (*Usnea longissima*). *Botany* **86**: 1224–1232.

Ronquist F, Huelsenbeck JP. 2003. MRBAYES 3: Bayesian phylogenetic inference under mixed models. *Bioinformatics* **19**:1572–1574.

Rosentreter R. 1993. Vagrant lichens in North America. *Bryologist* **96**: 333–338.

Rundel PW. 1978. Ecological relationships of desert fog zone lichens. *Bryologist* **81**: 277–293.

Rundel PW. 1982. The role of morphology in the water relations of desert lichens. *Journal of the Hattori Botanical Laboratory* **53**: 315–320.

Sancho LG, Kappen L. 1989. Photosynthesis and water relations and the role of anatomy in Umbilicaricaeae (Lichenes) from central Spain. *Oecologia* **81**: 473–480.

Sancho LG, Schroeter B, Del-Prado R. 2000. Ecophysiology and morphology of the globular erratic lichen *Aspicilia fruticulosa* (Eversm.) Flag. from central Spain. *Bibliotheca Lichenologica* **75**: 137–147.

Sanders WB, Ascaso C. 1995. Reiterative production and deformation of cell walls in expanding thallus nets of the lichen *Ramalina menziesii* (Lecanorales, Ascomycetes). *American Journal of Botany* **82**: 1358–1366.

Sanders WB. 2001. Lichens: the interface between mycology and plant morphology. *BioScience* **51**: 1025–1035.

Silvestro D, Michalak I. 2012. raxmlGUI: a graphical front-end for RAxML. *Organisms Diversity and Evolution*, in press. http://dx.doi.org/10.1007/s13127-011-0056-0.

Snelgar WP, Green TDA. 1981. Ecologically-linked variation in morphology, actyelene reduction, and water relations in *Pseudocyphellaria dissimilis*. *New Phytologist* **87**: 403–411.

Sojo F, Valladares F, Sancho LG. 1997. Structural and physiological plasticity of the lichen *Catillaria corymbosa* in different microhabitats of the maritime Antarctica. *Bryologist* **100**: 171–179.

Stamatakis A, Ludwig T, Meier H. 2005. RAxML-II: a program for sequential, parallel & distributed inference of large phylogenetic trees. *Concurrency and Computation: Practice and Experience* **17**: 1705–1723.

Sultan SE. 2000. Phenotypic plasticity for plant development, function, and life-history. *Trends in Plants Science* **5**: 537–542.

Thell A, Stenroos S, Feuerer T, Kärnefelt I, Myllys L, Hyvönen J. 2002. Phylogeny of cetrarioid lichens (Parmeliaceae) inferred from ITS and β-tubulin sequences, morphology, anatomy and secondary chemistry. *Mycological Progress* **1**: 335–354.

Thell A, Stenroos S, Myllys L. 2000. A DNA study of the *Cetraria aculeata* and *C. islandica* groups. *Folia Cryptogamica Estonica* **32**: 113–122.

Tretiach M, Brown DH. 1995. Morphological and physiological differences between epilithic and epiphytic populations of the lichen *Parmelia pastillifera*. *Annals of Botany* **75**: 627–632.

Valladares F, Gianoli E, Gómez JM. 2007. Ecological limits to plant phenotypic plasticity. *New Phytologist* **167**: 749–763.

Valladares F, Sancho LG, Ascaso C. 1998. Water storage in the lichen family Umbilicariaceae. *Botanica Acta* **111**: 99–107.

Valladares F, Ascaso C, Sancho LG. 1994. Intrathalline variability of some structural and physical parameters in the lichen genus *Lasallia*. *Canadian Journal of Botany* **72**: 415–428.

Valladares F. 1994. Texture and hygroscopic features of the upper surface of the thallus in the lichen family Umbilicariaceae. *Annals of Botany* **73**: 493–500.

Voisey CR. 2011. Intercalary growth in hyphae of filamentous fungi. *Fungal Biology Reviews* **24**: 123–131.

Weber WA. 1977. Environmental modification and lichen taxonomy. In: Seaward MRD. ed. *Lichen ecology*. London: Academic Press, 9–29.